AMERICAN SOCIETY FOR MICROBIOLOGY | Molecular and Cellular Biology

Identification of Novel Death-Associated Protein Kinase 2 Interaction Partners by Proteomic Screening Coupled with Bimolecular Fluorescence Complementation

Barbara Geering,[a] Zina Zokouri,[a] Samuel Hürlemann,[a] Bertran Gerrits,[c] David Ausländer,[a] Adrian Britschgi,[b] Mario P. Tschan,[b] Hans-Uwe Simon,[d] Martin Fussenegger[a,e]

Department of Biosystems Science and Engineering, ETH Zurich, Basel, Switzerland[a]; Institute of Pathology, University of Bern, Bern, Switzerland[b]; Functional Genomics Center Zurich, ETH Zurich, Zurich, Switzerland[c]; Institute of Pharmacology, University of Bern, Bern, Switzerland[d]; Faculty of Science, University of Basel, Basel, Switzerland[e]

Death-associated protein kinase 2 (DAPK2) is a Ca^{2+}/calmodulin-dependent Ser/Thr kinase that possesses tumor-suppressive functions and regulates programmed cell death, autophagy, oxidative stress, hematopoiesis, and motility. As only few binding partners of DAPK2 have been determined, the molecular mechanisms governing these biological functions are largely unknown. We report the identification of 180 potential DAPK2 interaction partners by affinity purification-coupled mass spectrometry, 12 of which are known DAPK binding proteins. A small subset of established and potential binding proteins detected in this screen was further investigated by bimolecular fluorescence complementation (BiFC) assays, a method to visualize protein interactions in living cells. These experiments revealed that α-actinin-1 and 14-3-3-β are novel DAPK2 binding partners. The interaction of DAPK2 with α-actinin-1 was localized at the plasma membrane, resulting in massive membrane blebbing and reduced cellular motility, whereas the interaction of DAPK2 with 14-3-3-β was localized to the cytoplasm, with no impact on blebbing, motility, or viability. Our results therefore suggest that DAPK2 effector functions are influenced by the protein's subcellular localization and highlight the utility of combining mass spectrometry screening with bimolecular fluorescence complementation to identify and characterize novel protein-protein interactions.

Death-associated protein kinases (DAPKs) are a family of five Ser/Thr kinases that share a high degree of sequence homology in their catalytic domains but differ significantly in their extracatalytic domains. The best-studied member of the DAPK family is DAPK1, a regulator of programmed cell death (1, 2), autophagy (3), and motility (4).

DAPK2 exhibits a kinase domain with 80% homology to the one of DAPK1 and also contains a calmodulin (CaM)-binding site (5, 6) but uniquely features a C-terminal homodimerization domain (6) while lacking the diverse protein-protein interaction domains that DAPK1 possesses (5, 6). The kinase is kept in an inactive conformation by a double-locking mechanism, which requires dephosphorylation of an autophosphorylated residue (Ser318) within the CaM-binding domain by a yet-to-be identified phosphatase in order to allow for CaM binding and homodimerization, both of which enhance kinase activity (7, 8). Also the phosphorylation of Ser299 by cyclic GMP (cGMP)-dependent protein kinase I (9) and the interaction with 14-3-3-τ (10) regulate DAPK2 kinase activity. To date, the only known DAPK2 substrates are DAPK2 itself, regulatory light chain of myosin II (RLC), and mammalian target of rapamycin complex 1 (mTORC1) (5, 6, 11).

DAPK2 was shown to mediate programmed cell death. Overexpression of DAPK2 results in morphological changes reminiscent of apoptosis in adherent cells, such as membrane blebbing and condensation of nuclei (5, 6), and in reduced viability and survival in suspension cells (12, 13). In line with these findings, restoration of DAPK2 activity through fusion of a constitutively active DAPK2 to CD30 in Hodgkin lymphoma cells resulted in selective apoptosis in tumor cells *in vitro* and in prolonged survival in a Hodgkin lymphoma mouse model (14), and depletion of DAPK2 sensitizes resistant cells to TRAIL-induced killing (15). DAPK2 also induces autophagy and autophagic cell death by directly interacting with mTORC1, one of the negative regulators of autophagy, and by suppressing its activity through phosphorylation (3, 11). Data from our laboratories further support a role for DAPK2 in immunity. We demonstrated that DAPK2 positively regulates the differentiation of innate immune cells (16) and boosts granulocyte chemotaxis by modulating cellular spreading and polarization (17). As granulocytes treated with DAPK2 inhibitors showed reduced migration toward the site of inflammation in a mouse model of peritonitis, DAPK2 may be a novel target for anti-inflammatory therapies (17). For a recent review on the regulatory role of DAPK2 on apoptosis, autophagy, and inflammation, see Geering (18).

In order to gain insight into the molecular mechanisms of DAPK2 biological functions, we identified potential DAPK2 interaction partners by coimmunoprecipitation assays followed by liquid chromatography-tandem mass spectrometry (LC-MS/MS). Out of 180 hits, 6 were chosen for further analysis by bimo-

Received 19 May 2015 **Returned for modification** 21 August 2015
Accepted 8 October 2015

Accepted manuscript posted online 19 October 2015

Citation Geering B, Zokouri Z, Hürlemann S, Gerrits B, Ausländer D, Britschgi A, Tschan MP, Simon H-U, Fussenegger M. 2016. Identification of novel death-associated protein kinase 2 interaction partners by proteomic screening coupled with bimolecular fluorescence complementation. Mol Cell Biol 36:132–143. doi:10.1128/MCB.00515-15.

Address correspondence to Barbara Geering, barbara.geering@bsse.ethz.ch.

Supplemental material for this article may be found at http://dx.doi.org/10.1128/MCB.00515-15.

lecular fluorescence complementation (BiFC). This method is based on the discovery that two nonfluorescent fragments of a fluorescent protein can form a fluorescent entity when in close proximity, for example, by fusion to interacting proteins. BiFC strategy was developed and utilized for a variety of applications, including the visualization of protein interactions (19), determination of subcellular localizations (20), and investigation of biological functions of protein-protein interactions (21). We applied BiFC to confirm and characterize the interaction of DAPK2 with the actin-binding protein α-actinin-1 and the scaffold protein 14-3-3-β.

We provide evidence that under steady-state conditions, DAPK2 localizes to the cytoplasm by interaction with 14-3-3-β, probably among other interaction partners. Upon cellular stimulation resulting in enhanced intracellular Ca^{2+} concentrations, DAPK2 binds to α-actinin-1, which is localized at the actin cortex adjacent to the plasma membrane. The association of DAPK2 with α-actinin-1 mediates increased membrane blebbing and reduced cellular motility. Hence, in our model, DAPK2 activity output is regulated by DAPK2 subcellular localization.

MATERIALS AND METHODS

Reagents. Cell culture reagents were purchased from PAA, buffer components were from Sigma, and in-gel digestion and LC solvents were from Rathburn.

Cell culture, transfection, and stimulation. NB4 cells (CSC-C0328; Creative Bioarray) were maintained in RPMI 1640 medium (E15-885; PAA) supplemented with 10% fetal calf serum (FCS) (2-01F10; Biochrom) and 1% penicillin-streptomycin (L0022; Biowest SAS) in a humidified 37°C incubator with 5% CO_2. HEK-293T (ATCC CRL_11268) and HeLa (ATCC CCL-2) cells were cultured in Dulbecco's modified Eagle's medium (DMEM) (52100-039; Life Technologies) supplemented with 10% FCS and 1% penicillin-streptomycin (complete DMEM) in a humidified 37°C incubator with 5% CO_2. At 20 h prior to transfection, 50,000 to 100,000 cells were seeded into 24-well plates containing 0.5 ml of complete DMEM. Cells were transfected with a 4:1 polyethylenimine-DNA (750 ng of total DNA) mix as previously described (22), and medium was changed to complete DMEM 7 h later. In order to increase intracellular Ca^{2+} concentrations, cells were treated with 1 μM ionomycin (BP2527-1; Fisher Scientific) for 1 h. Yellow fluorescent protein (YFP) fluorescence was usually assessed 24 to 48 h after transfection, and cells were grown at 30°C for at least 7 h prior to flow cytometry analysis.

Protein preparation for mass spectrometry. NB4 cells overexpressing CGW-FLAG-DAPK2 (16) were treated for 4.5 days with or without 1 μM all-*trans*-retinoic acid (ATRA) (A2169; Sigma) to induce differentiation. A total of 40×10^6 cells were lysed and preincubated with an antibody isotype control, followed by affinity purification using FLAG-IP (FLAG immunoprecipitation kit, FLAGIPT1; Sigma) according to the manufacturer's protocol. Immunoprecipitated proteins were separated by SDS-PAGE, and gels were fixed with 40% (vol/vol) ethanol–10% (vol/vol) acetic acid and stained with colloidal Coomassie blue G-250 (GelCode blue stain reagent, 24590; Pierce Biotechnology). Gel sections were cut into small pieces, washed three times with 50% acetonitrile, and dry spun. Ammonium bicarbonate (25 mM, pH 8) containing 300 ng of trypsin was added to each gel section and incubated at 37°C overnight. Tryptic peptides were extracted using 5% trifluoroacetic acid in 50% acetonitrile, and the samples were dried. Samples were resuspended in 1% acetonitrile–0.2% formic acid and subsequently desalted using ZipTip pipette tips (Merck Millipore).

Liquid chromatography-tandem mass spectrometry. Digests were analyzed on a Nano LC system (Eksigent Technologies) connected to a hybrid linear ion trap LTQ Orbitrap (Thermo Scientific), which was equipped with a nanoelectrospray ion source (Thermo Scientific). Peptide separation was carried out on a reverse-phase high-pressure liquid chromatography (RP-HPLC) column (75-μm inner diameter and 10-cm length) packed in-house with C_{18} resin (Magic C_{18} AQ, 3-μm particle size; Michrom Bioresources), using a linear gradient from 90% solvent A (water, 0.2% formic acid, and 1% acetonitrile) and 10% solvent B (water, 0.2% formic acid, and 80% acetonitrile) to 65% solvent A and 35% solvent B. The data acquisition mode was set to acquire one high-resolution MS scan followed by up to 10 data-dependent collision-induced dissociation MS/MS scans in the linear ion trap. Only MS signals exceeding 500 ion counts triggered an MS/MS attempt, and 10^4 ions were acquired for an MS/MS scan over a maximum time of 200 ms. The normalized collision energy was set to 35%. Singly charged ions were excluded from triggering MS/MS scans.

MS data analysis. Tandem mass spectra were extracted, charge state deconvoluted, and deisotoped by Mascot Distiller, version 2.2. All MS/MS samples were analyzed using Mascot (version 2.2.04; Matrix Science, London, United Kingdom). Mascot was set up to search the human portion of the UniProt database (56,722 entries, including common contaminants; February 2009) assuming the digestion enzyme trypsin. Mascot was searched with a fragment ion mass tolerance of 0.8 Da and a parent ion tolerance of 10 ppm. The following variable modifications were specified in Mascot: Gln → pyro-Glu of the N terminus, deamidated of asparagine and glutamine, and oxidation of methionine. Scaffold (Scaffold_4.4.1; Proteome Software, Inc., Portland, OR) was used to validate MS/MS-based peptide and protein identifications. Peptide identifications were accepted if they could be established at greater than 95.0% probability by the Peptide Prophet algorithm (23) with a Scaffold delta-mass correction. Protein identifications were accepted if they could be established at greater than 99.0% probability and contained at least two identified peptides. Protein probabilities were assigned by the Protein Prophet algorithm (24). Proteins that contained similar peptides and could not be differentiated based on MS/MS analysis alone were grouped to satisfy the principles of parsimony. Proteins sharing significant peptide evidence were grouped into clusters. Only proteins with 10 or more unique peptide counts were taken into consideration; keratin contaminants were excluded.

Vector design for BiFC assays. DNA sequences for the N terminus (amino acids 1 to 154) and C terminus (amino acids 155 to 238) of YFP (YFP_N and YFP_C, respectively; split YFP) including a linker region and XhoI or ApaI restriction enzyme site, were synthesized by GenScript (see the supplemental material). cDNA encoding DAPK2 was described previously (16). cDNA encoding CaM (plasmid 20435), α-actinin (plasmid 11908), 14-3-3-β (plasmid 13270), glucose-6-phosphate 1-dehydrogenase (G6PD; plasmid 41521), and signal-induced proliferation-associated protein (SIPA; plasmid 38154) was purchased from Addgene. cDNA was amplified with the respective primers containing an XhoI or ApaI restriction site. Restricted fragments were cloned into pcDNA3.1(+) (Life Technologies). Digested linker-YFP sequences were subsequently cloned into the constructs containing the protein of interest in pcDNA3.1(+), resulting in 5′-YFP-linker-cDNA-3′ or 5′-cDNA-linker-YFP-3′ constructs (more detailed information is given in Table S2 in the supplemental material). As DAPK2 proteins homodimerize, DAPK2-YFP_N and DAPK2-YFP_C were used as positive controls. Enhanced YFP (eYFP)-containing pcDNA3.1(+) was used as a transfection control. Plasmids containing the split YFP constructs (YFP_N and YFP_C) were used as negative controls.

Flow cytometry. Cells were analyzed in an LSR Fortessa instrument (BD Bioscience) using BD FACSDiva software. YFP fluorescence was analyzed in nonfixed cells. Cellular viability was assessed after uptake of 5 μg/ml propidium iodide as previously described (25). Data were analyzed by FlowJo (Tree Star, Inc.).

Confocal microscopy. Subcellular localization of YFP fluorescence was analyzed on a Leica confocal laser scanning TCS SP5 microscope. Cells were seeded on poly-D-lysine (P7280; Sigma)-coated glass dishes (Fluorodish) and analyzed using 20× and 40× objectives. Fluorescence intensity graphs were extracted using ImageJ (http://imagej.nih.gov/ij/), and data were analyzed using Prism (GraphPad).

ELISA. Direct interactions between DAPK2 and α-actinin-1 or 14-3-3-β and DAPK2 kinase activities were tested by enzyme-linked immunosorbent assay (ELISA). For the assessment of direct interactions, high-binding 96-well plates (3590; Costar) were coated with 0.5 to 10 μg/ml recombinant protein in phosphate-buffered saline (PBS) (0.5 μg/ml recombinant DAPK2 [PV3614; Life Technologies], 5 μg/ml recombinant α-actinin-1 [ab152166; Abcam], and 1 to 2 μg/ml recombinant 14-3-3-β [ab78683; Abcam]) overnight at 4°C and blocked with 1% bovine serum albumin (BSA). To assess the interaction between DAPK2 and α-actinin-1, 1 μg/ml DAPK2 in protein kinase buffer (B6022S; NEB) containing 100 nM CaM (208670; Millipore) and/or 10 μM $CaCl_2$ was added for 3 h to α-actinin-1-coated wells. To assess the interaction between DAPK2 and 14-3-3-β, 1 μg/ml DAPK2 in kinase buffer containing 10 μM ATP (FLAAS; Sigma) was added for 3 h to 14-3-3-β-coated wells. Binding of DAPK2 to the coated interaction partners was assessed using anti-DAPK2 antibodies (1:1,000) (GTX61602; GeneTex) and horseradish peroxidase (HRP)-coupled anti-rabbit IgG (1:5,000) (7074; Cell Signaling Technology), followed by addition of 1-Step ABTS [2,2′-azinobis(3-ethylbenzthiazolinesulfonic acid)] (37615; Thermo Scientific). Absorbance at 405 nm was measured using an Infinite M200 Pro microplate reader (Tecan). For the assessment of DAPK2 activity, 0.3 μg/ml recombinant RLC (pro-366; Prospect) was coated onto high-binding 96-well plates overnight at 4°C and blocked with 1% BSA, and 2.5 μg/ml DAPK2 was added in kinase buffer containing 10 μM ATP. To test any effects of α-actinin-1 or 14-3-3-β on DAPK2 activity toward RLC, 6.76 μg/ml α-actinin-1 and 1.46 μg/ml 14-3-3-β were added to DAPK2 before addition to RLC. Phosphorylation of RLC was assessed using anti-phospho-RLC antibody (1:1,000) (3674; Cell Signaling) and HRP-coupled anti-rabbit IgG (1:5,000), followed by addition of 1-Step ABTS and measurement of absorbance as described above.

Scratch assay. In order to investigate the motility of HEK-293T and HeLa cells, migration of cells to a scratched area was assessed by microscopy. To this end, 200,000 HeLa cells were transfected with split YFP constructs and transferred to wells coated with poly-D-lysine (100 μg/ml) (P7280; Sigma). The following morning, a 10-μl pipette tip was used to introduce a scratch across the well, and two images per scratch were taken every hour by time-lapse microscopy using a wide-field Nikon eclipse Ti. The wound area at each time point was then extracted by the MatLab plug-in Qu. For analysis, the slope of a linear fit of the change in area from 5 to 20 h was extracted and compared between samples.

Statistical analysis. All data are shown as means ± standard deviations (SD) and were analyzed by paired Student *t* test unless indicated otherwise; *n* is defined as the number of independent experiments performed.

RESULTS

Unbiased identification of potential DAPK2 interaction partners by LC-MS/MS. In order to identify novel interaction partners of DAPK2, we chose to apply mass spectrometry analyses to proteins pulled down together with DAPK2. As DAPK2 was previously shown to mediate neutrophil differentiation and chemotaxis (16, 17), differentiated neutrophils were used for this experimental setup. FLAG-tagged DAPK2 protein was overexpressed in NB4 myeloid precursor cells, and the cells were incubated with all-*trans*-retinoic acid (ATRA) in order to differentiate the cells to neutrophil-like entities. Cell lysates of differentiated DAPK2-overexpressing NB4 cells were prepared, and DAPK2 was pulled down using anti-FLAG antibodies coupled to agarose resin. Immunoprecipitated proteins were separated by SDS-PAGE (Fig. 1A). The gel lanes were sectioned as shown, and the content was analyzed by LC-MS/MS. Proteins identified with more than 10 unique peptide hits were included in the analysis. This resulted in the identification of 180 potential DAPK2 interaction partners (see Table S1 in the supplemental material), 12 of which are known DAPK interaction partners (Table 1). Many cytoskeletal and signaling proteins were detected, which made up one-third of all proteins identified in association with DAPK2, as shown in Fig. 1B. This observation is in agreement with previously identified DAPK interaction partners that are either cytoskeletal proteins, including actin and tubulin, or proteins associated with the cytoskeleton, such as myosin II, cofilin, and tropomyosin. Interestingly, many proteins localizing to the nucleus were also identified in this screen, suggesting that DAPK2 may enter this compartment although its distribution is generally considered to be cytoplasmic (6). This finding may be explained by the recent identification of an alternatively spliced DAPK2 isoform called DRP-1β (26). DRP-1β lacks the Ca^{2+}/calmodulin-binding and homodimerization domain of DAPK2 and instead possesses a leucine zipper domain highly homologous to that of DAPK3, possibly allowing it to interact with nuclear proteins containing leucine zippers.

Confirmation of DAPK2 homodimerization and interaction with CaM by BiFC. In subsequent experiments, bimolecular fluorescence complementation (BiFC) was used to validate potential protein interactions (Fig. 2A). In the chosen setup, the N-terminal sequence of YFP (YFP_N; amino acids 1 to 154) was fused to one potential interaction partner, the C-terminal sequence of YFP (YFP_C; amino acids 155 to 238) was fused to the other potential interaction partner, and the complementary split YFP constructs were coexpressed within cells. In a first step, YFP_N and YFP_C were thus fused to the N or C terminus of DAPK2 and CaM, two known DAPK2 interaction partners, which were also identified in our mass spectrometry screen (Table 1), resulting in YFP_N-DAPK2, YFP_C-DAPK2, DAPK2-YFP_N, DAPK2-YFP_C, CaM-YFP_N, and CaM-YFP_C constructs (see Table S2 in the supplemental material). Because granulocytes are notoriously difficult to genetically manipulate (27), we used the human HEK-293T or HeLa cell line for further experiments. As shown in the upper panel of Fig. 2B, transfection of control constructs YFP_N and YFP_C (lacking fusion proteins that may trigger their association) into HEK-293T cells resulted in minor fluorescence detected by flow cytometry compared to that in cells transfected with the full-length YFP gene. As the proportion of HEK-293T cells transfected with the full-length YFP gene fluctuated between 40% and 60% of the whole population from one experiment to the next, we always analyzed YFP fluorescence of controls or potential interaction partners relative to this positive control, i.e., full-length YFP.

Transfection of two complementary split YFP-DAPK2 constructs (Fig. 2B) or a complementary split YFP-DAPK2 and complementary split YFP-CaM construct (Fig. 2C) resulted in at least twice as many HEK-293T cells positive for YFP fluorescence than observed for split YFP control constructs, with similar results seen in HeLa cells (data not shown), confirming the utility of BiFC to investigate DAPK2 interaction partners. YFP fluorescence of split YFP constructs was much increased when cells were cultured for at least 7 h at 30°C prior to analysis compared to levels in cells that were kept at 37°C, as previously described (see Fig. S1A in the supplemental material) (28). While decreasing the amount of DNA transfected into HEK-293T cells reduced YFP fluorescence of split YFP control constructs, the YFP fluorescence of split YFP-DAPK2 constructs also decreased (see Fig. S1B). The best fluorescence ratios between control and DAPK2 homodimers were observed when 50,000 HEK-293T cells were transfected with 250 ng of each construct. Interestingly, transfection of N-terminal fu-

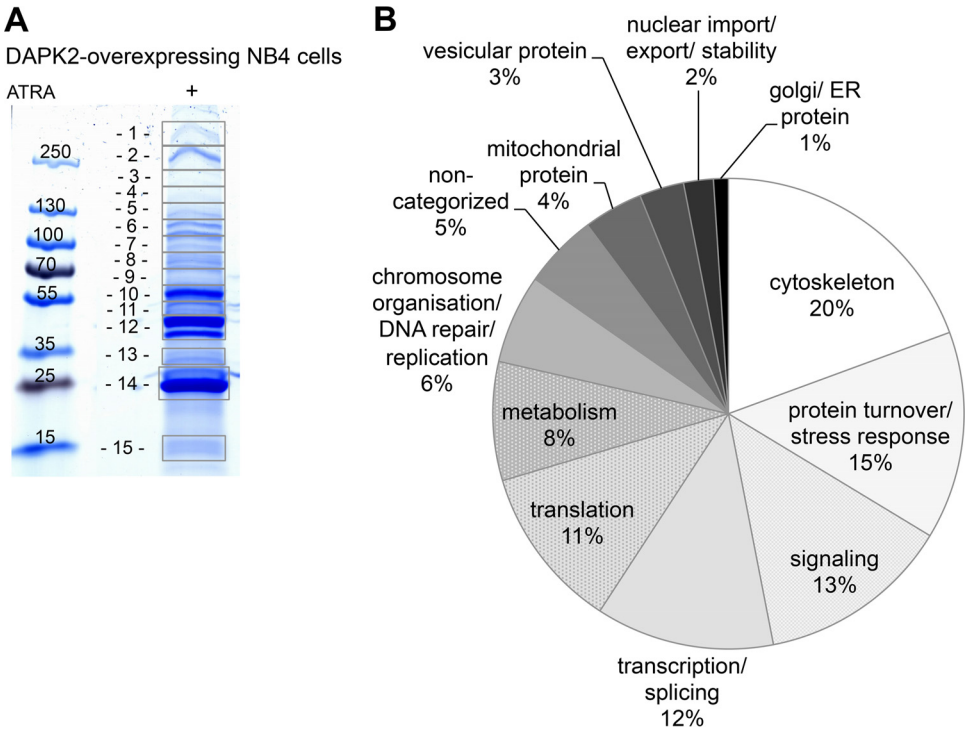

FIG 1 Identification of novel DAPK2 interaction partners by coimmunoprecipitation experiments and LC-MS/MS. (A) Colloidal Coomassie-stained SDS-PAGE showing gel sections (1 to 15) to be identified by LC-MS/MS. DAPK2-overexpressing NB4 cells were treated with 1 μM ATRA for 4.5 days, DAPK2 was immunoprecipitated from cell lysates, and proteins were separated by SDS-PAGE. Potential DAPK2 interaction partners were stained with colloidal Coomassie blue, and gel slices were cut as indicated for subsequent LC-MS/MS analysis ($n = 1$). (B) The majority of potential DAPK2 interaction partners are involved in cytoskeletal rearrangements, stress response, or signaling. Proteins identified by LC-MS/MS with a minimum of 10 matching queries were clustered into 12 main categories. Potential interaction partners are listed in Table S1 in the supplemental material.

sions of split YFP to DAPK2 (YFP_N-DAPK2 and YFP_C-DAPK2) resulted in higher YFP fluorescence than C-terminal YFP fusions (DAPK2-YFP_N and DAPK2-YFP_C), indicating that YFP at the C terminus of DAPK2 may interfere with homodimerization (Fig. 2B, lower panel), leading to decreased fluorescence. In contrast, transfection of N- or C-terminal fusions of split YFP to DAPK2 resulted in similar YFP fluorescence levels when CaM was coexpressed in HEK-293T cells, indicating that CaM binding to DAPK2 is not disturbed by an N- or a C-terminal YFP tag (Fig. 2C, lower panel).

Validation of novel interaction partners α-actinin-1 and 14-3-3-β by BiFC and ELISA. We chose to analyze the potential interaction of DAPK2 with four unrelated proteins, α-actinin-1, 14-3-3-β, signal-induced proliferation-associated protein 1 (SIPA), and glucose-6-phosphate 1-dehydrogenase (G6PD), all of which were identified with higher prevalence in an LC-MS/MS screen

TABLE 1 Known DAPK interaction partners identified[a]

UniProt accession no.	Description	Sequence coverage (%)	No. of unique peptides identified	Mol mass (kDa)	Gel section (no.)	Interacting DAPK family member(s)	Reference(s)
CALM_HUMAN	Calmodulin	81	11	17	15	DAPK1, -2, -3	1
COF1_HUMAN	Cofilin	42	5	18	15	DAPK1	41
DAPK2_HUMAN	Death-associated protein kinase 2	48	22	43	1 to 15	DAPK2	6
HS90B_HUMAN	HSP90	40	26	90	6	DAPK1, -2, -3	42
B4DWW4_HUMAN	DNA replication licensing factor MCM3	13	12	96	6	DAPK1	43
MRLC2_HUMAN	Myosin regulatory light chain	40	6	20	15	DAPK1, -2, -3	1
KPYM_HUMAN	Pyruvate kinase isoform M2	42	19	58	7, 8, 9	DAPK1	44
MYPT1_HUMAN	Protein phosphatase 1 regulatory subunit	24	27	115	5	DAPK3	45
TPM3_HUMAN	Tropomyosin	46	16	29	13	DAPK1	46
Q5JP53_HUMAN	Tubulin, beta	52	16	48	10, 11	DAPK1	47
1433B_HUMAN	14-3-3-β	61	13	28	13, 14	DAPK1	35
1433T_HUMAN	14-3-3-τ	44	13	27	13, 14	DAPK1, -2	10, 35

[a] A mass spectrometry screen to identify potential DAPK2 interaction partners was undertaken by ectopic expression of DAPK2 in NB4 cells. DAPK2 protein was immunoprecipitated from cell lysates and separated by SDS-PAGE. Gel sections were excised and proteins were analyzed by LC-MS/MS. Twelve known DAPK interaction partners were identified.

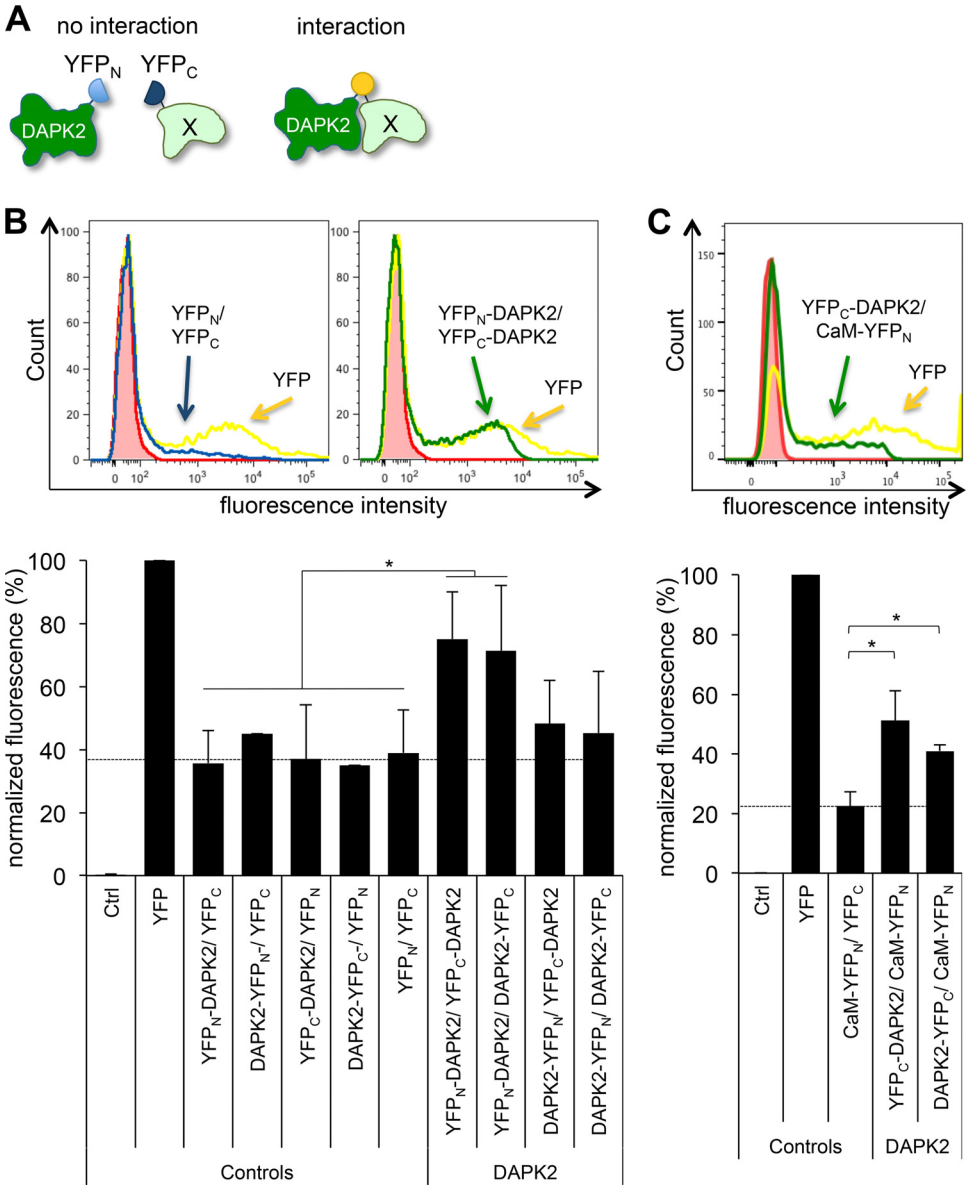

FIG 2 Validation of bimolecular fluorescence complementation (BiFC) for the analysis of DAPK2 interaction partners. (A) Schematic representation of the principle underlying BiFC. DAPK2 and potential interaction partner X are fused to either of two split YFP fragments (YFP$_N$ or YFP$_C$). If no interaction occurs between the proteins, no or little mature YFP will form. If DAPK2 interacts with protein X, the split YFP fragments will join and mature to a fluorescent entity. (B) N-terminal fusion of split YFP constructs to DAPK2 allows for the detection of fluorescence above background due to DAPK2 homodimerization. Relative fluorescence of HEK-293T cells was analyzed by flow cytometry following ectopic expression of split YFP or full-length YFP constructs in order to assess usability of BiFC for investigation of potential DAPK2 interaction partners. Representative flow cytometry histograms of cells expressing full-length YFP or control constructs (left) and full-length YFP and split YFP constructs (right) are shown in the upper panels. The lower panel shows a quantitative analysis of fluorescent cells containing full-length YFP (set as 100) or split YFP constructs ($n \geq 3$). (C) Increased fluorescence in HEK-293T cells coexpressing split YFP constructs and DAPK2 and CaM. The upper panels shows a representative flow cytometry histogram of cells expressing full-length YFP and split YFP constructs. The lower panel shows a quantitative analysis of fluorescent cells containing full-length YFP (set as 100) or split YFP constructs ($n = 4$).

(see Table S1 in the supplemental material). As shown in Fig. 3A, YFP fluorescence was increased in cells coexpressing split YFP–α-actinin-1 and -DAPK2 as well as split YFP–14-3-3-β and -DAPK2 constructs compared to levels in control cells expressing split YFP–α-actinin-1 or –14-3-3-β and YFP$_N$, respectively. Similar results were obtained when HeLa cells were cotransfected with different split YFP constructs (see Fig. S2 in the supplemental material). Increased YFP fluorescence was not observed in HEK-293T cells cotransfected with split YFP-G6PD and -DAPK2 or split YFP-SIPA and -DAPK2. These data therefore suggested that α-actinin-1 and 14-3-3-β are novel interaction partners of DAPK2 (in the meantime, 14-3-3-β was independently confirmed to be a DAPK2 interaction partner [29]).

Because DAPK2 activity can be increased by Ca^{2+} levels through binding of and activation by Ca^{2+}-bound CaM, we further assessed whether the interaction of DAPK2 with α-actinin-1, G6PD, SIPA, or 14-3-3-β was influenced by intracellular Ca^{2+} concentrations. To this end, HEK-293T cells expressing split YFP

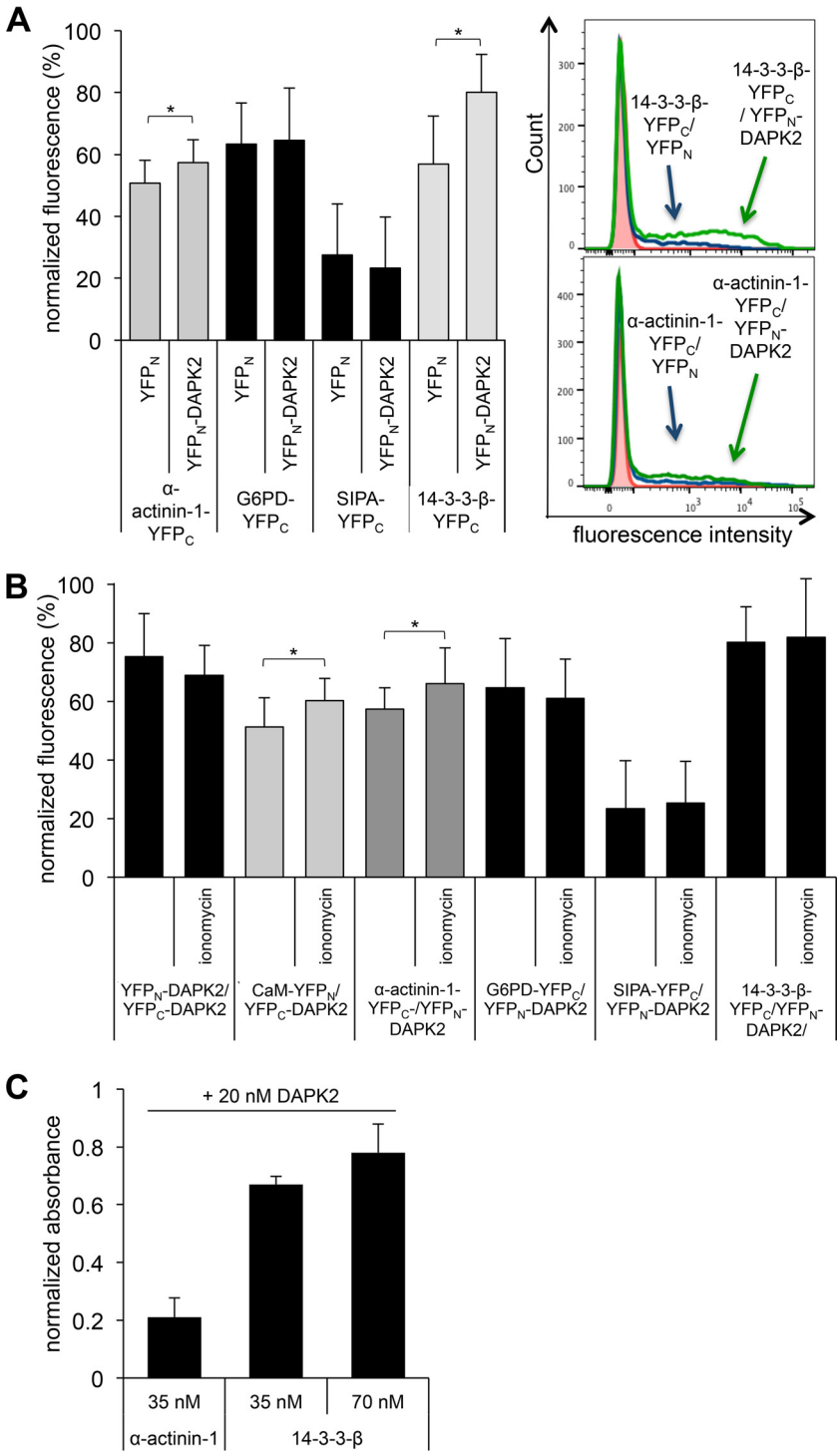

FIG 3 Confirmation of novel DAPK2 interaction partners α-actinin-1 and 14-3-3-β by BiFC. (A) DAPK2 interacts with α-actinin-1 and 14-3-3-β under steady-state conditions. A significant increase in fluorescence could be observed after coexpression of split YFP constructs YFP_N-DAPK2 and α-actinin-1–YFP_C and of YFP_N-DAPK2 and 14-3-3-β–YFP_C in HEK-293T cells. Ectopic expression of split YFP constructs YFP_N-DAPK2 and G6PD-YFP_C or SIPA-YFP_C did not increase fluorescence above background levels ($n = 8$). (B) Increased intracellular Ca^{2+} levels due to ionomycin treatment augments association of DAPK2 with α-actinin-1. Treatment of HEK-293T cells with 1 μM ionomycin for 1 h resulted in increased fluorescence of cells ectopically expressing split YFP construct YFP_N-DAPK2 and α-actinin-1–YFP_C and also YFP_C-DAPK2 and CaM-YFP_N, measured by flow cytometry 24 h later ($n \geq 3$). (C) Direct interaction of DAPK2 with α-actinin-1 and 14-3-3-β. Recombinant human α-actinin-1 (35 nM) and 14-3-3-β (35 and 70 nM) were coated onto ELISA plates and incubated with 20 nM recombinant human DAPK2. Absolute absorbance values of noncoated wells were subtracted from absolute absorbance values of coated wells, resulting in relative absorbance, shown in this graph ($n = 3$).

constructs were treated with ionomycin, an ionophore potently increasing intracellular Ca^{2+} levels, and YFP fluorescence was assessed by flow cytometry (Fig. 3B). Indeed, ionomycin treatment resulted in small, but significantly increased, fluorescence in cells cotransfected with split YFP-DAPK2 and -CaM or –α-actinin-1 but not with any other construct. These data suggest that elevated Ca^{2+} levels, as occurring after cellular stimulation, drive the interaction of DAPK2 with CaM, as previously shown (5, 6), and also that with the newly identified α-actinin-1.

In order to assess whether α-actinin-1 and 14-3-3-β are direct binding partners of DAPK2, recombinant human α-actinin-1 and 14-3-3-β were coated onto high-affinity plastic plates, and the interaction with recombinant human DAPK2 was analyzed by using anti-DAPK2 antibodies (indirect ELISA method). As shown in Fig. 3C, an interaction of α-actinin-1 with DAPK2 could be observed when similar molarities of DAPK2 and α-actinin-1 were added. The interaction was not increased in the presence of Ca^{2+} or Ca^{2+}-loaded CaM (data not shown), suggesting that the elevated interaction between α-actinin-1 and DAPK2 upon ionomycin treatment was based on more parameters than just increased Ca^{2+} concentrations. Equally, interaction of 14-3-3-β and DAPK2 was detected by ELISA and was independent of DAPK2 autophosphorylation as addition of ATP and kinase buffer to DAPK2, allowing for increased DAPK2 kinase activity, did not have an impact on the interaction (data not shown). In summary, the interaction of DAPK2 with α-actinin-1 and 14-3-3-β was observed by BiFC *in cellulo* and by ELISA *in vitro*.

Interaction of DAPK2 with α-actinin-1 results in massive blebbing and decreased migration. DAPK2 was previously shown to trigger cellular blebbing, programmed cell death, and motility when ectopically expressed (5, 6, 17). We therefore analyzed whether the newly identified interaction partners might have an impact on any of these properties. As endogenous DAPK2 expression levels are hardly detectable by immunoblotting (data not shown), we assumed that ectopically expressed DAPK2 would mainly interact with ectopically expressed interaction partners. Overexpression of split YFP-DAPK2 constructs YFP_N-DAPK2 and YFP_C-DAPK2 (leading to DAPK2 homodimerization) indeed resulted in 30% of cells with a blebbing phenotype compared to levels in cells overexpressing split YFP only and also compared to levels in cells expressing only one copy of DAPK2 (Fig. 4A), suggesting that the blebbing phenotype depends on DAPK2 expression levels and/or homodimerization. Expression of split YFP-DAPK2 and -CaM or –α-actinin-1 greatly enhanced the number of cells with a blebbing phenotype compared to levels in control cells, with the majority of cells demonstrating a blebbing phenotype following ectopic expression of split YFP–α-actinin-1 and -DAPK2. In contrast, similar numbers of cells with a blebbing phenotype were observed when the interaction of split YFP-DAPK2 with –14-3-3-β compared to that in control cells was analyzed, contrary to previous reports in cells overexpressing DAPK2 and 14-3-3-τ, which showed reduced levels of blebbing (10). Expression of a split YFP construct fused to an inactive DAPK2 mutant (YFP_N-K52A and YFP_C-K52A) resulted in only a few blebbing cells in combination with split YFP-DAPK2, -CaM and –14-3-3-β, suggesting that DAPK2 activity was essential for the observed phenotype. Although overexpression of split YFP–α-actinin-1 together with YFP_N-K52A reduced the number of blebbing cells significantly compared to levels in cells expressing split YFP–α-actinin-1 with DAPK2 and also without DAPK2, residual blebbing suggests that α-actinin-1 also mediates blebbing independent of DAPK2 activity.

Blebbing is associated with diverse cellular properties, among others, cell death. In order to assess whether DAPK2 overexpression would induce cell death that might be accompanied by blebbing as previously observed (5, 6), we measured the uptake of propidium iodide at 48 h (see Fig. S3 in the supplemental material) and 72 h (data not shown) after transfection. Although viability of the cell population generally decreased over time as expected, we could not observe any significant difference between the numbers of necrotic cells in the diverse cell samples, independent of intracellular Ca^{2+} levels. As only 6% of split YFP transfected cells stained positive for annexin V at 48 h after transfection (data not shown), these data suggest that cells overexpressing split YFP-DAPK2 and depicting a blebbing phenotype are mostly viable.

Both DAPK1 and DAPK2 were shown to regulate cellular motility. Whereas DAPK1 negatively regulates migration of cells by interfering with integrin signaling (30), DAPK2 positively regulates migration by acting on spreading and polarization (17). Here, we used a scratch assay to investigate whether DAPK2 homodimerization or its interaction with CaM, α-actinin-1, or 14-3-3-β would have an impact on cellular migration. To this end, the closure of a wound in a monolayer of HeLa cells was followed by time-lapse wide-field microscopy (Fig. 4B; see also Fig. S4 in the supplemental material). Quantification of the changes in cell-free area over time revealed that ectopic expression of two complementary split YFP-DAPK2 constructs (YFP_N-DAPK2 and YFP_C-DAPK2), leading to DAPK2 homodimerization, indeed resulted in cells with increased migration compared to levels in cells expressing control constructs, in line with previous reports that inhibition of DAPK2 activity slows down cellular motility (17). Expression of split YFP-DAPK2 and -CaM or –α-actinin-1, however, caused the cells to move more slowly, resulting in reduced closure of the wound. Overexpression of split YFP–14-3-3-β in combination with split YFP-DAPK2 had no apparent impact on cellular migration. These differences in wound closure were not due to changes in doubling times as proliferation was not affected by ectopic expression of split YFP constructs (data not shown). Our data therefore suggest that ectopic expression of split YFP-DAPK2 constructs leading to DAPK2 homodimerization results in moderate levels of cellular blebbing and increased migration. Interaction of DAPK2 with CaM or α-actinin-1 mediates a more pronounced blebbing phenotype and reduced migration. These observations indicate an inverse correlation between the blebbing phenotype and cellular motility mediated by DAPK2.

Interaction of DAPK2 with α-actinin-1 localizes DAPK2 to the plasma membrane. The data presented in Fig. 4 indicate that DAPK2 kinase activity was increased by homodimerization, CaM binding, and α-actinin-1 interaction. As recombinant α-actinin-1 did not increase recombinant DAPK2 kinase activity toward recombinant RLC *in vitro* (data not shown), we hypothesized that DAPK2 subcellular localization may be crucial for the phenotype observed. One of the major advantages of using BiFC for the identification of protein-protein interactions is the possibility to concomitantly investigate the distribution of the interaction within a cell. Hence, we assessed the localization of DAPK2 interacting with DAPK2, CaM, α-actinin-1, and 14-3-3-β using the split YFP constructs. As shown in Fig. 5A (upper panels) and B, the interaction of DAPK2 with all of these proteins but α-actinin-1 re-

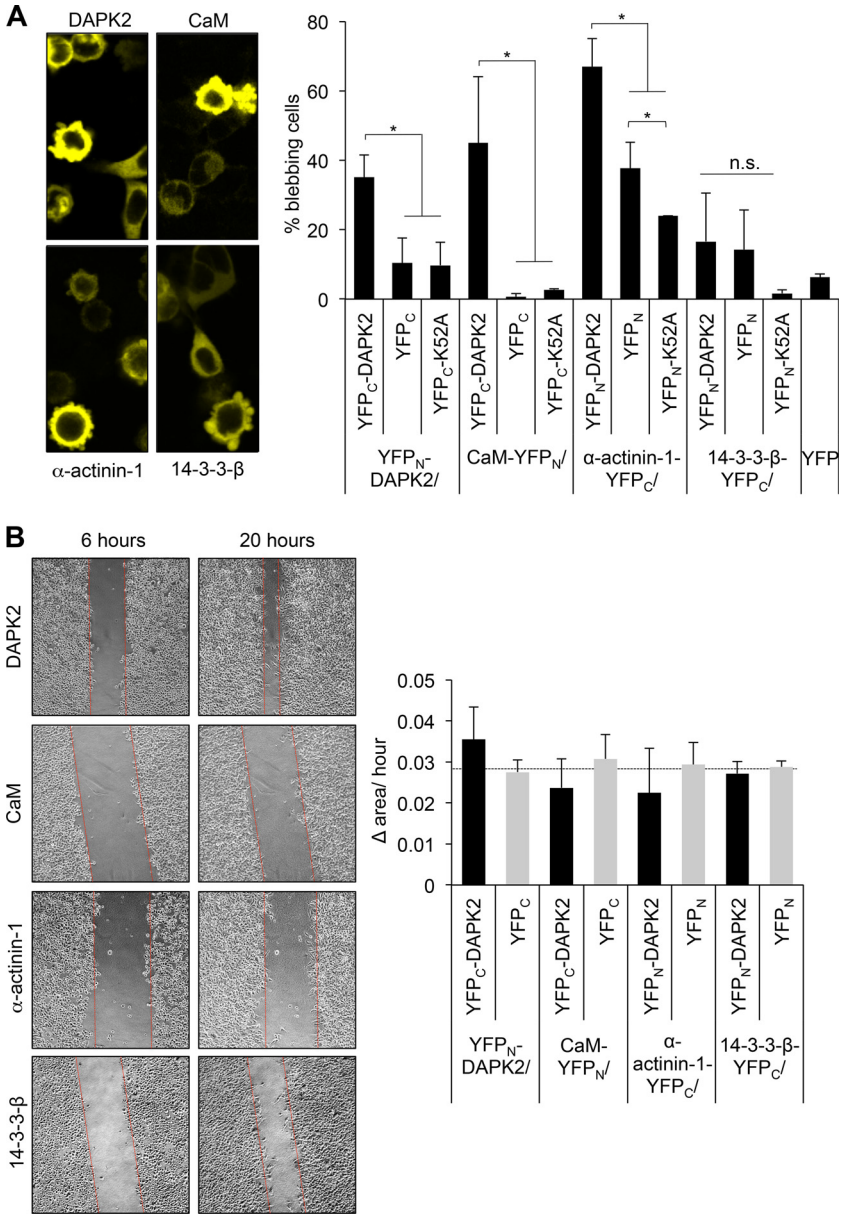

FIG 4 Interaction of DAPK2 with α-actinin-1 increases cellular blebbing and reduces motility. (A) Ectopic expression of DAPK2 augments cellular blebbing in HEK-293T cells. Representative confocal images of split YFP-expressing cells (left) and quantitative analysis of the blebbing phenotype associated with DAPK2 overexpression (right) are shown. Split YFP constructs of DAPK2 wild type and an inactive mutant (K52A) were coexpressed with split YFP constructs and CaM, α-actinin-1, and 14-3-3-β. At least 100 fluorescent cells were counted for each sample in each experiment ($n = 4$). (B) Interaction of DAPK2 with α-actinin-1 dampens motility in HeLa cells. Cells expressing split YFP constructs were seeded onto a poly-D-lysine-coated surface and grown to confluence. A scratch was introduced at time point 0, and migration was investigated by time-lapse microscopy for the following 24 h, with two pictures taken per scratch and duplicate every hour. The left panel shows representative wide-field images at time points 6 and 20 h after introduction of the scratch. The right panel shows quantitative analysis of wound closure within the linear range over time (the slope of a linear fit of the change in area, Δ area/h) for HeLa cells expressing split YFP constructs ($n = 2$).

vealed a mainly cytoplasmic distribution. Also, the background fluorescence of the interaction partners with control constructs was localized to the cytoplasm (Fig. 5A, lower panel). In contrast, DAPK2 binding to α-actinin-1 was localized at the plasma membrane. These data reveal that homodimerization of DAPK2 and its interaction with CaM and 14-3-3-β are localized mainly to the cytoplasm although in highly blebbing cells, YFP fluorescence was also observed at the plasma membrane. The interaction of DAPK2 with α-actinin-1, however, occurs at the plasma membrane, suggesting that relocalization of DAPK2 to the actin cortex upon binding to α-actinin-1 may bring the kinase in close proximity to its substrates, resulting in increased blebbing.

DISCUSSION

A total of 168 potentially novel DAPK2 interaction partners were identified by using an unbiased LC-MS/MS approach. The association of DAPK2 with two of these, namely, α-actinin-1 and 14-3-3-β, was characterized in detail. We concentrated our investi-

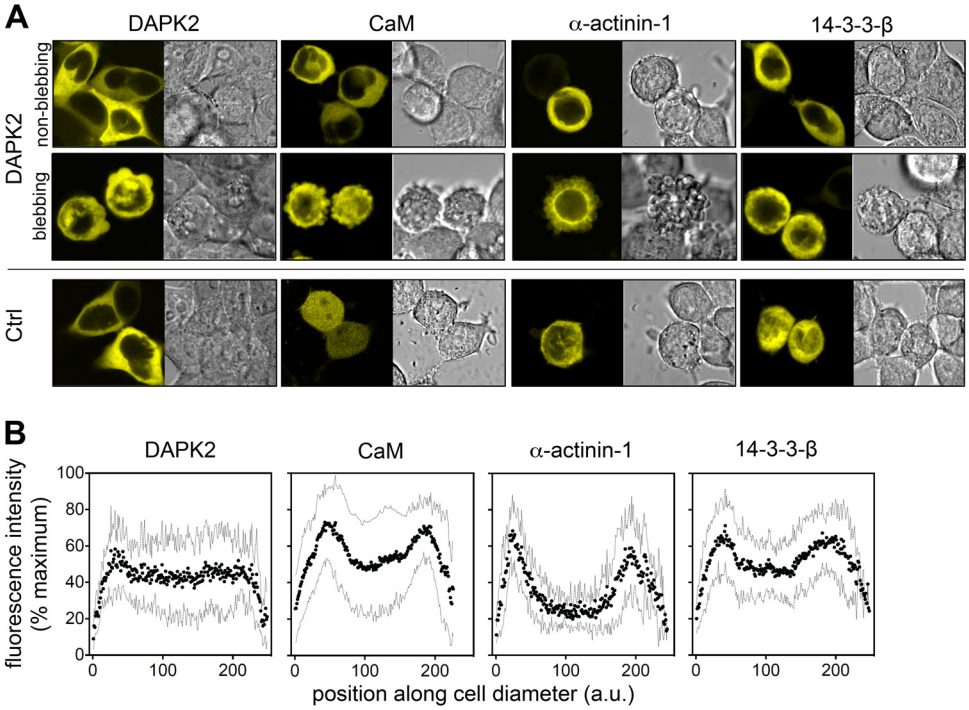

FIG 5 Forced interaction of DAPK2 with α-actinin-1 mediates relocalization of DAPK2 to the plasma membrane. (A) Confocal fluorescence images of HEK-293T cells expressing split YFP constructs and DAPK2, CaM, α-actinin-1, and 14-3-3-β (upper panel) and controls thereof (lower panel). (B) Quantification of fluorescence intensity along the cell diameter. Ten randomly chosen cells were profiled for their fluorescence intensity along their diameter using ImageJ, and the data were normalized and quantified using GraphPad Prism ($n = 4$). a.u., arbitrary units.

gations on α-actinin-1 because this protein was identified with high prevalence by the mass spectrometry screen, suggesting that α-actinin-1 was binding tightly and/or at a high molar ratio to DAPK2. In addition, α-actinin-4, α-spectrin, and β-spectrin, three members of the same family of actin-binding proteins, were also identified in the top 20 interaction partners of the mass spectrometry screen, indicating that motifs common to these family members, for example, the CaM homology domain (31), may be responsible for the interaction. As α-actinin-1 not only cross-links actin bundles into stress fibers but also interacts with integrins to mediate connection between the cytoskeleton and plasma membrane (32) and is mainly localized to the contractile actin cortex (33), binding of DAPK2 to α-actinin-1 would provide a presently missing link between DAPK2 and its substrate RLC, localized at the plasma membrane. In addition, 14-3-3-β was chosen for further investigations because, as for α-actinin-1, the protein was identified with high prevalence by LC-MS/MS. Furthermore, 14-3-3-β, which is a phospho-Ser/phospho-Thr binding protein with a vast variety of functions (34), was previously shown to interact with DAPK1 in hippocampal areas surviving a seizure (35), and 14-3-3-β and 14-3-3-τ have recently been demonstrated to interact with phosphorylated DAPK2 (10, 29).

Using two independent approaches to confirm the association of α-actinin-1 and 14-3-3-β with DAPK2, we provide solid evidence of the validity of these novel interaction partners. On the one hand, the potential interactions were confirmed *in cellulo* by a BiFC approach, used to identify and localize interaction and study biological functions thereof (28). Whereas YFP fluorescence upon ectopic expression of split YFP–α-actinin-1 and -DAPK2 constructs under steady-state conditions was only slightly, but significantly, increased compared to the levels of the split YFP control constructs in HEK-293T cells, an 80% increase in fluorescence was observed when split YFP–α-actinin-1 was coexpressed with split YFP-DAPK2 in HeLa cells compared to levels in split YFP controls, suggesting cell-type-specific differences in the association. Following elevation of intracellular Ca^{2+} by ionomycin treatment of HEK-293T cells, the interaction of α-actinin-1 and DAPK2 was elevated to a similar extent as the binding between CaM and DAPK2 increased in the presence of Ca^{2+}, indicating that these associations may be intensified upon cellular stimulation. Given that α-actinin-1 and α-actinin-4 were shown to interact with the CaM-binding domain of binding partners (36), we hypothesized that the CaM-binding domain of DAPK2 may be responsible for increased α-actinin-1 binding upon ionomycin treatment. Indeed, coexpression of a split YFP-CaM-deficient DAPK2 mutant with split YFP–α-actinin-1 resulted in decreased fluorescence in a BiFC assay (data not shown), suggesting that α-actinin-1 binds to DAPK2 through the CaM-binding motif. Also the interaction of split YFP-DAPK2 with split YFP–14-3-3-β was investigated by analyzing changes in YFP fluorescence and was found to be increased by more than 30% in HEK-293T and HeLa cells compared to that in cells expressing split YFP control constructs. Yet no impact on the interaction by ionomycin treatment could be observed, indicating that this association may occur independent of cellular stimulation.

On the other hand, the interactions between DAPK2 and α-actinin-1 or 14-3-3-β were analyzed *in vitro* using an ELISA. Indeed, recombinant α-actinin-1 was shown to interact directly with recombinant DAPK2. To our surprise, the *in vitro* interaction was independent of Ca^{2+} or Ca^{2+}/CaM, in contrast to results obtained

in ionomycin-treated cells. This may be due to additional effects of ionomycin treatment on cellular signaling that cannot be recapitulated *in vitro*, allowing for increased DAPK2 and α-actinin-1 interaction. Also, 14-3-3-β interacted directly with DAPK2 and, interestingly, independent of any phosphorylated residue. As 14-3-3-β and 14-3-3-τ have been shown to interact with a Ser/Thr-rich stretch at the very C terminus of DAPK2 only when these residues were phosphorylated (10, 29), our data suggesting that binding of DAPK2 with 14-3-3-β may also occur through different molecular mechanisms may be reminiscent of the interaction of 14-3-3-β with DAPK1 (35).

We furthermore demonstrate that the interaction of DAPK2 with α-actinin-1 and 14-3-3-β affects the subcellular localization of DAPK2. DAPK2 was shown to be localized to the cytoplasm (6), and confocal microscopy of cells expressing split YFP-DAPK2 constructs, leading to DAPK2 homodimerization, confirm these data. We also observed cytoplasmic distribution of DAPK2 in association with CaM and 14-3-3-β. However, confocal microscopy of cells ectopically expressing split YFP-DAPK2 and –α-actinin-1 constructs revealed a localization of DAPK2 to the plasma membrane when DAPK2 associated with α-actinin-1. As α-actinin-1 is part of the contractile cell cortex localized at the inner phase of the plasma membrane, localization of DAPK2 to α-actinin-1 and hence to the actin cortex may allow for interaction of DAPK2 with its substrate RLC, which is known to interact with the actin cytoskeleton.

Finally, our data provide evidence that the regulation of blebbing (5, 6) and motility (17) by DAPK2 may, in fact, be due to the interaction of DAPK2 with α-actinin-1. During blebbing, the contractile cortex rich in actin filaments, myosin II, and actin-binding proteins (37) detaches from the plasma membrane, allowing the generation of plasma membrane extrusion. As expansion ceases, contractile cortex reassembles under the membrane and drives bleb retraction (38). This bleb retraction was shown to be mediated by myosin II activation (39). Ectopic expression of split YFP-DAPK2 and –α-actinin-1 results in more than 70% of the fluorescent cell population producing blebs. Using different control constructs, we could show that the phenotype is caused to a large extent by active DAPK2 interacting with α-actinin-1, with a small proportion of blebbing being DAPK2 independent.

Myosin II activation is also crucial for cellular motility. Whereas actin polymerization is driving the cell to move forward, myosin-mediated contractile forces help to detach and pull the rear. We have previously observed that inactivation of DAPK2 by small-molecule inhibitors dampens motility of granulocytes toward chemoattractants (17). Here, we provide evidence that overexpression of DAPK2 results in increased migration in HeLa cells. However, while low levels of blebbing seem to support or even mediate motility (40), our data suggest that when a large proportion of the cell population undergoes massive blebbing, migration is reduced. These data may also indicate that the level of DAPK2 activity determines whether a cell will move more quickly or more slowly.

To our surprise, we did not observe any effect of DAPK2 overexpression on cellular viability although DAPK2 is considered a regulator of apoptosis and although its overexpression was previously shown to mediate cell death (5, 6). This discrepancy may be explained by differences in analytical methods to identify dying cells. Hence, early publications mainly investigated death by analyzing morphological properties such as blebbing, which may occur independent of cell death, whereas we assessed cellular death by determining the percentage of cells with permeabilized membranes. In line with this, we previously did not find any correlation between DAPK2 kinase activity and cellular viability (17), and DAPK2 depletion was recently shown to sensitize cells to TRAIL-induced apoptosis (15). Furthermore, the amount of DAPK2 overexpressed in cells may also be crucial for the observation of DAPK2-mediated phenotypes. We used 250 ng and 500 ng of DAPK2-containing plasmid to transfect 50,000 cells and could observe a blebbing phenotype only with the latter amount. Previously, 750 ng (3, 6) or 1,000 ng (5) of DAPK2-containing plasmid was used to transfect the same number of cells, resulting in blebbing and nuclear condensation. Our data thus indicate that a fine-tuned balance of DAPK2 activity may regulate cellular viability.

In summary, we provide evidence about two novel DAPK2 binding partners, α-actinin-1 and 14-3-3-β, that may regulate DAPK2 activity by modulating its subcellular localization. Interaction of DAPK2 with 14-3-3-β is localized to the cytoplasm and is independent of cellular stimulation. This interaction has no apparent effect on cellular blebbing, viability, or migration. In contrast, the interaction of DAPK2 with α-actinin-1 is increased by cellular stimulation and localizes DAPK2 to the cell surface. Binding of DAPK2 to α-actinin-1 results in increased blebbing and reduced migration. Our data thus provide insight into the regulation of DAPK2 activity.

ACKNOWLEDGMENTS

We thank Aaron Ponti, Erica Montani, Verena Jäggin, and Thomas Horn for invaluable technical support.

FUNDING INFORMATION

L'Oréal for Women in Science provided funding to Barbara Geering. INTERREG IV A.20 provided funding to Martin Fussenegger. Cancer Research Switzerland provided funding to Mario P. Tschan under grant number KFS-3409-02-2014.

REFERENCES

1. **Cohen O, Feinstein E, Kimchi A.** 1997. DAP-kinase is a Ca^{2+}/calmodulin-dependent, cytoskeletal-associated protein kinase, with cell death-inducing functions that depend on its catalytic activity. EMBO J **16:**998–1008. http://dx.doi.org/10.1093/emboj/16.5.998.
2. **Chen CH, Wang WJ, Kuo JC, Tsai HC, Lin JR, Chang ZF, Chen RH.** 2005. Bidirectional signals transduced by DAPK-ERK interaction promote the apoptotic effect of DAPK. EMBO J **24:**294–304. http://dx.doi.org/10.1038/sj.emboj.7600510.
3. **Inbal B, Bialik S, Sabanay I, Shani G, Kimchi A.** 2002. DAP kinase and DRP-1 mediate membrane blebbing and the formation of autophagic vesicles during programmed cell death. J Cell Biol **157:**455–468. http://dx.doi.org/10.1083/jcb.200109094.
4. **Wang WJ, Kuo JC, Yao CC, Chen RH.** 2002. DAP-kinase induces apoptosis by suppressing integrin activity and disrupting matrix survival signals. J Cell Biol **159:**169–179. http://dx.doi.org/10.1083/jcb.200204050.
5. **Kawai T, Nomura F, Hoshino K, Copeland NG, Gilbert DJ, Jenkins NA, Akira S.** 1999. Death-associated protein kinase 2 is a new calcium/calmodulin-dependent protein kinase that signals apoptosis through its catalytic activity. Oncogene **18:**3471–3480. http://dx.doi.org/10.1038/sj.onc.1202701.
6. **Inbal B, Shani G, Cohen O, Kissil JL, Kimchi A.** 2000. Death-associated protein kinase-related protein 1, a novel serine/threonine kinase involved in apoptosis. Mol Cell Biol **20:**1044–1054. http://dx.doi.org/10.1128/MCB.20.3.1044-1054.2000.
7. **Shani G, Henis-Korenblit S, Jona G, Gileadi O, Eisenstein M, Ziv T,**

Admon A, Kimchi A. 2001. Autophosphorylation restrains the apoptotic activity of DRP-1 kinase by controlling dimerization and calmodulin binding. EMBO J **20:**1099–1113. http://dx.doi.org/10.1093/emboj/20.5.1099.

8. **Shohat G, Shani G, Eisenstein M, Kimchi A.** 2002. The DAP-kinase family of proteins: study of a novel group of calcium-regulated death-promoting kinases. Biochim Biophys Acta **1600:**45–50. http://dx.doi.org/10.1016/S1570-9639(02)00443-0.
9. **Isshiki K, Matsuda S, Tsuji A, Yuasa K.** 2012. cGMP-dependent protein kinase I promotes cell apoptosis through hyperactivation of death-associated protein kinase 2. Biochem Biophys Res Commun **422:**280–284. http://dx.doi.org/10.1016/j.bbrc.2012.04.148.
10. **Gilad Y, Shiloh R, Ber Y, Bialik S, Kimchi A.** 2014. Discovering protein-protein interactions within the programmed cell death network using a protein-fragment complementation screen. Cell Rep **8:**909–921. http://dx.doi.org/10.1016/j.celrep.2014.06.049.
11. **Ber Y, Shiloh R, Gilad Y, Degani N, Bialik S, Kimchi A.** 2015. DAPK2 is a novel regulator of mTORC1 activity and autophagy. Cell Death Differ **22:**465–475. http://dx.doi.org/10.1038/cdd.2014.177.
12. **Britschgi A, Simon HU, Tobler A, Fey MF, Tschan MP.** 2010. Epigallocatechin-3-gallate induces cell death in acute myeloid leukaemia cells and supports all-trans retinoic acid-induced neutrophil differentiation via death-associated protein kinase 2. Br J Haematol **149:**55–64. http://dx.doi.org/10.1111/j.1365-2141.2009.08040.x.
13. **Fang J, Menon M, Zhang D, Torbett B, Oxburgh L, Tschan M, Houde E, Wojchowski DM.** 2008. Attenuation of EPO-dependent erythroblast formation by death-associated protein kinase-2. Blood **112:**886–890. http://dx.doi.org/10.1182/blood-2008-02-138909.
14. **Tur MK, Neef I, Jager G, Teubner A, Stocker M, Melmer G, Barth S.** 2009. Immunokinases, a novel class of immunotherapeutics for targeted cancer therapy. Curr Pharm Des **15:**2693–2699. http://dx.doi.org/10.2174/138161209788923877.
15. **Schlegel CR, Fonseca AV, Stocker S, Georgiou ML, Misterek MB, Munro CE, Carmo CR, Seckl MJ, Costa-Pereira AP.** 2014. DAPK2 is a novel modulator of TRAIL-induced apoptosis. Cell Death Differ **21:**1780–1791. http://dx.doi.org/10.1038/cdd.2014.93.
16. **Rizzi M, Tschan MP, Britschgi C, Britschgi A, Hugli B, Grob TJ, Leupin N, Mueller BU, Simon HU, Ziemiecki A, Torbett BE, Fey MF, Tobler A.** 2007. The death-associated protein kinase 2 is up-regulated during normal myeloid differentiation and enhances neutrophil maturation in myeloid leukemic cells. J Leukoc Biol **81:**1599–1608. http://dx.doi.org/10.1189/jlb.0606400.
17. **Geering B, Stoeckle C, Rozman S, Oberson K, Benarafa C, Simon HU.** 2014. DAPK2 positively regulates motility of neutrophils and eosinophils in response to intermediary chemoattractants. J Leukoc Biol **95:**293–303. http://dx.doi.org/10.1189/jlb.0813462.
18. **Geering B.** 2015. Death-associated protein kinase 2: regulator of apoptosis, autophagy and inflammation. Int J Biochem Cell Biol **65:**151–154. http://dx.doi.org/10.1016/j.biocel.2015.06.001.
19. **Hu CD, Chinenov Y, Kerppola TK.** 2002. Visualization of interactions among bZIP and Rel family proteins in living cells using bimolecular fluorescence complementation. Mol Cell **9:**789–798. http://dx.doi.org/10.1016/S1097-2765(02)00496-3.
20. **Citovsky V, Lee LY, Vyas S, Glick E, Chen MH, Vainstein A, Gafni Y, Gelvin SB, Tzfira T.** 2006. Subcellular localization of interacting proteins by bimolecular fluorescence complementation in planta. J Mol Biol **362:**1120–1131. http://dx.doi.org/10.1016/j.jmb.2006.08.017.
21. **Kodama Y, Hu CD.** 2012. Bimolecular fluorescence complementation (BiFC): a 5-year update and future perspectives. Biotechniques **53:**285–298. http://dx.doi.org/10.2144/000113943.
22. **Auslander D, Eggerschwiler B, Kemmer C, Geering B, Auslander S, Fussenegger M.** 2014. A designer cell-based histamine-specific human allergy profiler. Nat Commun **5:**4408. http://dx.doi.org/10.1038/ncomms5408.
23. **Keller A, Nesvizhskii AI, Kolker E, Aebersold R.** 2002. Empirical statistical model to estimate the accuracy of peptide identifications made by MS/MS and database search. Anal Chem **74:**5383–5392. http://dx.doi.org/10.1021/ac025747h.
24. **Nesvizhskii AI, Keller A, Kolker E, Aebersold R.** 2003. A statistical model for identifying proteins by tandem mass spectrometry. Anal Chem **75:**4646–4658. http://dx.doi.org/10.1021/ac0341261.
25. **Geering B, Simon HU.** 2011. A novel signaling pathway in TNFα-induced neutrophil apoptosis. Cell Cycle **10:**2821–2822. http://dx.doi.org/10.4161/cc.10.17.16747.
26. **Shoval Y, Berissi H, Kimchi A, Pietrokovski S.** 2011. New modularity of DAP-kinases: alternative splicing of the DRP-1 gene produces a ZIPk-like isoform. PLoS One **6:**e17344. http://dx.doi.org/10.1371/journal.pone.0017344.
27. **Geering B, Schmidt-Mende J, Federzoni E, Stoeckle C, Simon HU.** 2011. Protein overexpression following lentiviral infection of primary mature neutrophils is due to pseudotransduction. J Immunol Methods **373:**209–218. http://dx.doi.org/10.1016/j.jim.2011.08.024.
28. **Kerppola TK.** 2006. Design and implementation of bimolecular fluorescence complementation (BiFC) assays for the visualization of protein interactions in living cells. Nat Protoc **1:**1278–1286. http://dx.doi.org/10.1038/nprot.2006.201.
29. **Yuasa K, Ota R, Matsuda S, Isshiki K, Inoue M, Tsuji A.** 2015. Suppression of death-associated protein kinase 2 by interaction with 14-3-3 proteins. Biochem Biophys Res Commun **464:**70–75. http://dx.doi.org/10.1016/j.bbrc.2015.05.105.
30. **Kuo JC, Wang WJ, Yao CC, Wu PR, Chen RH.** 2006. The tumor suppressor DAPK inhibits cell motility by blocking the integrin-mediated polarity pathway. J Cell Biol **172:**619–631. http://dx.doi.org/10.1083/jcb.200505138.
31. **Winder SJ, Hemmings L, Maciver SK, Bolton SJ, Tinsley JM, Davies KE, Critchley DR, Kendrick-Jones J.** 1995. Utrophin actin binding domain: analysis of actin binding and cellular targeting. J Cell Sci **108:**63–71.
32. **Pavalko FM, Otey CA, Simon KO, Burridge K.** 1991. Alpha-actinin: a direct link between actin and integrins. Biochem Soc Trans **19:**1065–1069. http://dx.doi.org/10.1042/bst0191065.
33. **Otey CA, Carpen O.** 2004. Alpha-actinin revisited: a fresh look at an old player. Cell Motil Cytoskeleton **58:**104–111. http://dx.doi.org/10.1002/cm.20007.
34. **Morrison DK.** 2009. The 14-3-3 proteins: integrators of diverse signaling cues that impact cell fate and cancer development. Trends Cell Biol **19:**16–23. http://dx.doi.org/10.1016/j.tcb.2008.10.003.
35. **Henshall DC, Araki T, Schindler CK, Shinoda S, Lan JQ, Simon RP.** 2003. Expression of death-associated protein kinase and recruitment to the tumor necrosis factor signaling pathway following brief seizures. J Neurochem **86:**1260–1270. http://dx.doi.org/10.1046/j.1471-4159.2003.01934.x.
36. **Hall DD, Dai S, Tseng PY, Malik Z, Nguyen M, Matt L, Schnizler K, Shephard A, Mohapatra DP, Tsuruta F, Dolmetsch RE, Christel CJ, Lee A, Burette A, Weinberg RJ, Hell JW.** 2013. Competition between α-actinin and Ca^{2+}-calmodulin controls surface retention of the L-type Ca^{2+} channel $Ca_V1.2$. Neuron **78:**483–497. http://dx.doi.org/10.1016/j.neuron.2013.02.032.
37. **Charras GT, Hu CK, Coughlin M, Mitchison TJ.** 2006. Reassembly of contractile actin cortex in cell blebs. J Cell Biol **175:**477–490. http://dx.doi.org/10.1083/jcb.200602085.
38. **Bovellan M, Fritzsche M, Stevens C, Charras G.** 2010. Death-associated protein kinase (DAPK) and signal transduction: blebbing in programmed cell death. FEBS J **277:**58–65. http://dx.doi.org/10.1111/j.1742-4658.2009.07412.x.
39. **Charras GT, Coughlin M, Mitchison TJ, Mahadevan L.** 2008. Life and times of a cellular bleb. Biophys J **94:**1836–1853. http://dx.doi.org/10.1529/biophysj.107.113605.
40. **Charras G, Paluch E.** 2008. Blebs lead the way: how to migrate without lamellipodia. Nat Rev Mol Cell Biol **9:**730–736. http://dx.doi.org/10.1038/nrm2453.
41. **Ivanovska J, Tregubova A, Mahadevan V, Chakilam S, Gandesiri M, Benderska N, Ettle B, Hartmann A, Soder S, Ziesche E, Fischer T, Lautscham L, Fabry B, Segerer G, Gohla A, Schneider-Stock R.** 2013. Identification of DAPK as a scaffold protein for the LIMK/cofilin complex in TNF-induced apoptosis. Int J Biochem Cell Biol **45:**1720–1729. http://dx.doi.org/10.1016/j.biocel.2013.05.013.
42. **Zhang L, Nephew KP, Gallagher PJ.** 2007. Regulation of death-associated protein kinase. Stabilization by HSP90 heterocomplexes. J Biol Chem **282:**11795–11804.
43. **Bialik S, Berissi H, Kimchi A.** 2008. A high throughput proteomics screen identifies novel substrates of death-associated protein kinase. Mol Cell Proteomics **7:**1089–1098. http://dx.doi.org/10.1074/mcp.M700579-MCP200.

44. **Mor I, Carlessi R, Ast T, Feinstein E, Kimchi A.** 2012. Death-associated protein kinase increases glycolytic rate through binding and activation of pyruvate kinase. Oncogene **31:**683–693. http://dx.doi.org/10.1038/onc.2011.264.
45. **Takamoto N, Komatsu S, Komaba S, Niiro N, Ikebe M.** 2006. Novel ZIP kinase isoform lacks leucine zipper. Arch Biochem Biophys **456:**194–203. http://dx.doi.org/10.1016/j.abb.2006.09.026.
46. **Houle F, Poirier A, Dumaresq J, Huot J.** 2007. DAP kinase mediates the phosphorylation of tropomyosin-1 downstream of the ERK pathway, which regulates the formation of stress fibers in response to oxidative stress. J Cell Sci **120:**3666–3677. http://dx.doi.org/10.1242/jcs.003251.
47. **Harrison B, Kraus M, Burch L, Stevens C, Craig A, Gordon-Weeks P, Hupp TR.** 2008. DAPK-1 binding to a linear peptide motif in MAP1B stimulates autophagy and membrane blebbing. J Biol Chem **283:**9999–10014. http://dx.doi.org/10.1074/jbc.M706040200.